A New Heuristic UTD Diffraction Coefficient for Nonperfectly Conducting Wedges

Peter D. Holm

***Abstract*—A new heuristic UTD diffraction coefficient for nonperfectly conducting wedges is proposed. The coefficient is an extension of the heuristic one given by Luebbers and as simple as that to compute. In the case of forward-scattering and neglecting the surface wave effects, the new coefficient gives a result close to Maliuzhinets's solution, also deep in the shadow region where the previous one fails. Moreover, it makes the special care used by Luebbers to deal with grazing incidence unnecessary.**

***Index Terms*—Diffraction coefficients, geometrical theory of diffraction, nonperfectly conducting surfaces.**

I. Introduction

PROPAGATION over irregular terrain is a complex problem but is of interest when it comes to siting ground links, for instance. In order to find practical solutions, simplifying assumptions are required. One approach is to apply the uniform geometrical theory of diffraction (GTD) [1] to a piecewise-linear terrain profile. Besides a piecewise approximation of the terrain, this theory requires the scattering events to be local phenomena, i.e., independent. For large distances compared to the wavelength, typically several hundred wavelengths, this condition is thoroughly satisfied. On the other hand, to ensure this, the terrain profile has to be approximated with only a few piecewise-linear segments. Even so, some good results have been reported [2]–[5].

The advantage of a piecewise-linear terrain profile is in the application of available solutions for diffraction by a wedge that are numerically efficient. In 1962, Keller formulated the GTD and an enclosed wedge diffraction coefficient [6]. This original coefficient is numerically simple but not valid in the vicinity of shadow and reflection boundaries, i.e., boundaries where direct and reflected rays, respectively, appear or disappear. The one used today is valid in the vicinity of shadow and reflection boundaries and still quite numerically efficient to evaluate. This coefficient was formulated by Kouyoumjian and Pathak in 1974 [7] and resulted in a uniform theory, the uniform geometrical theory of diffraction (UTD), which is valid everywhere in space as long as the incident fields are ray optical and reflection and diffraction events can be considered local phenomena.

The diffraction coefficient in [7] is for wedges with perfectly conducting surfaces. Wedge diffraction solutions for nonperfectly conducting surfaces are available [8]–[14], but many of these are based on Maliuzhinets's solution [8] and are rather cumbersome to use. The special function introduced by Maliuzhinets [8] is difficult to calculate for an arbitrary wedge angle, so these solutions are not practical for path-loss predictions over real terrain due to the complexity of the problem.

The difficulties of using rigorous solutions for path-loss predictions over real terrain force simplifications to be made. In [2]–[5], the heuristic diffraction coefficient formulated in [3] is used. This coefficient, which does not account for surface waves, is efficient to evaluate. Moreover, when neglecting surface wave effects, it will give results close to Maliuzhinets's solution in the vicinity of the reflection boundaries [15], [16]. However, in the shadow region, it generally gives a diffracted field that does not agree very well with Maliuzhinets's solution [16], [17], especially deep in the shadow region. In this paper, a solution that agrees very well with Maliuzhinets's solution in the shadow region is proposed. The solution is heuristic and not formally based on Maxwell's equations. The result, however, is very convincing.

II. Theory

The ray method UTD (or GTD) uses basically three kinds of rays: direct, reflected, and diffracted rays [1]. The diffracted rays are multiplied by diffraction coefficients (and proper spreading factors) and the coefficient for diffraction by a wedge reads as [1], [7]

$$D = D(L, n; \phi, \phi') = D^{(1)} + D^{(2)} + R_0 D^{(3)} + R_n D^{(4)} \quad (1)$$

where R_0 and R_n are the reflection coefficients for the zero- and n-face, respectively (see Fig. 1). For perfectly conducting surfaces, $R_{0,n}$ is -1 for soft (horizontal) and $+1$ for hard (vertical) polarization. The components $D^{(l)}$ ($l = 1, 2, 3, 4$) of the diffraction coefficient in (1) are given by

$$\begin{aligned} D^{(l)} &= D^{(l)}(L, n; \phi, \phi') \\ &= \frac{-e^{-j\pi/4}}{2n\sqrt{2\pi k}} \cot \gamma^{(l)} F_0\left(2kLn^2 \sin^2 \gamma^{(l)}\right) \end{aligned} \quad (2)$$

where

k	wave number;
L	$s's/(s'+s)$;
$n\pi$	exterior angle of the wedge;
F_0	transition function defined in [7];
$\gamma^{(1)}$	$[\pi - (\phi - \phi')]/2n$;
$\gamma^{(2)}$	$[\pi + (\phi - \phi')]/2n$;
$\gamma^{(3)}$	$[\pi - (\phi + \phi')]/2n$;
$\gamma^{(4)}$	$[\pi + (\phi + \phi')]/2n$.

Here, as in [18], we use the result put forward in [19] and [20], which removes the integer $N^{\pm}$ defined by Kouyoumjian and

Manuscript received July 29, 1998; revised April 26, 2000.

The author is with the Department of Communication Systems, Division of Command and Control Warfare Technology, Defence Research Establishment, SE-581 11 Linköping, Sweden.

Publisher Item Identifier S 0018-926X(00)06940-4.

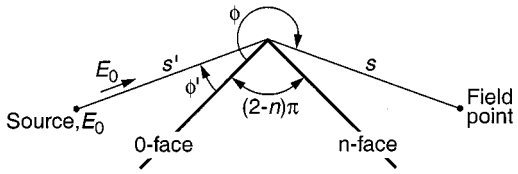

Fig. 1. Ray geometry for diffraction by a noncurved wedge.

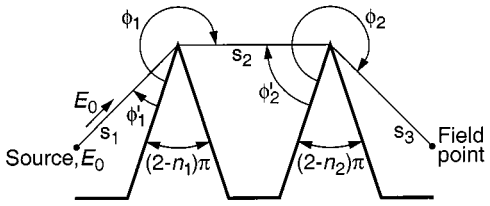

Fig. 2. Ray geometry for diffraction by two noncurved wedges.

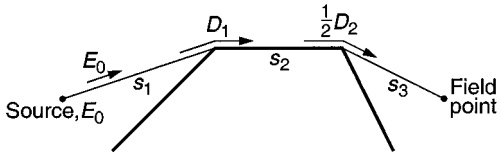

Fig. 3. Diffraction by two joined wedges when using a factor of 1/2 for grazing incidence.

Pathak [7]. As far as we know, this does not give a significantly different result. Instead, it means some computational simplifications.

The basic idea of the UTD is that diffracted rays can be treated in the same way as reflected rays in the geometrical optics (GO), i.e., diffraction events can be seen as independent local phenomena. The field of the diffracted ray in Fig. 1 can be written straightforwardly as [1]

$$E_{\mathrm{UTD}} = E^{\mathrm{i}} D \sqrt{\frac{s'}{s(s'+s)}}\, e^{-jks} \tag{3}$$

where

$$E^{\mathrm{i}} = \frac{E_0 e^{-jks'}}{s'} \tag{4}$$

is the field incident on the wedge, and E_0 the relative amplitude of a spherical source; or in a more compact form as

$$E_{\mathrm{UTD}} = \frac{E_0 e^{-jks_{\mathrm{T}}}}{s_{\mathrm{T}}} D \sqrt{\frac{s_{\mathrm{T}}}{s's}} \tag{5}$$

where $s_{\mathrm{T}} = s' + s$ is the total path distance. Here, we have assumed spherical waves. However, by altering spreading factors, the calculations or the expressions can be made valid for other waves, such as plane or cylindrical waves [7]. Furthermore, an $\exp^{+j\omega t}$ time dependence has been implicitly assumed and suppressed throughout.

Now, if the diffraction events can be seen as local phenomena, the field of the doubly diffracted ray in Fig. 2 can directly be written as [1], [18]

$$E_{\mathrm{UTD}} = E_2^{\mathrm{i}} D_2 \sqrt{\frac{s_1+s_2}{s_3\,(s_1+s_2+s_3)}}\, e^{-jks_3} \tag{6}$$

where

$$E_2^{\mathrm{i}} = E_1^{\mathrm{i}} D_1 \sqrt{\frac{s_1}{s_2\,(s_1+s_2)}}\, e^{-jks_2} \tag{7}$$

is the field incident on the second wedge

$$E_1^{\mathrm{i}} = \frac{E_0 e^{-jks_1}}{s_1} \tag{8}$$

is the field incident on the first wedge and D_1 and D_2 are the diffraction coefficients of the first and the second wedge, respectively; or in a more compact form as

$$E_{\mathrm{UTD}} = \frac{E_0 e^{-jks_{\mathrm{T}}}}{s_{\mathrm{T}}} D_1 D_2 \sqrt{\frac{s_{\mathrm{T}}}{s_1 s_2 s_3}} \tag{9}$$

where $s_{\mathrm{T}} = s_1 + s_2 + s_3$ is the total path distance. Furthermore, for the sake of simplicity, the arguments of D_1 and D_2 are suppressed here and assumed to be understood.

The field in (6) or in (9) is the first-order diffracted field of the ray in Fig. 2 and gives a good enough result if $s_2 \gg s_1$, s_3 and ks_1, ks_2, $ks_3 \gg 1$ are satisfied. The latter condition is fundamental for a high-frequency method such as the UTD, at least if one expects the theory to give a reliable result. Furthermore, the additional condition $s_2 \gg s_1$, s_3 ensures that higher order diffracted fields are negligible (see Appendix). If this is not the case, higher order fields might contribute, even though ks_1, ks_2, $ks_3 \gg 1$. If so, they have to be included, which results in the field [18]

$$E_{\mathrm{UTD}} = \frac{E_0 e^{-jks_{\mathrm{T}}}}{s_{\mathrm{T}}} \sqrt{\frac{s_{\mathrm{T}}}{s_1 s_2 s_3}} \sum_{m=0}^{\infty} \frac{1}{m!} \left(\frac{-1}{jks_2}\right)^m \cdot \frac{\partial^m D_1}{\partial \phi_1^m} \frac{\partial^m D_2}{\partial \phi_2'^m} \tag{10}$$

for the ray in Fig. 2, where the first-order diffracted field is the term $m = 0$. Here, one may note that diffraction events are not local if (10) has to be used, which is not in line with the basic idea of the UTD, or the GO, where scattering events are considered to be independent. Thus, by using (10), one is able to cling to a picture that, to some extent, has broken down. Note: there is a misprint in [18]; [18, eq. (14)] should read as (10) in this paper.

A special case of double diffraction will be considered in this paper. The case is illustrated in Fig. 3. Here, the second wedge is illuminated at grazing incidence by the field from the first wedge. The factor of 1/2 in Fig. 3 is used in order to handle the special case of grazing incidence [1], [7]. Moreover, this multiplying factor has become accepted practice for perfectly conducting surfaces.

III. Heuristic Diffraction Coefficient by Luebbers

The diffraction coefficient in (1) is formulated for diffraction by a wedge with perfectly conducting faces. In [3], a heuristic

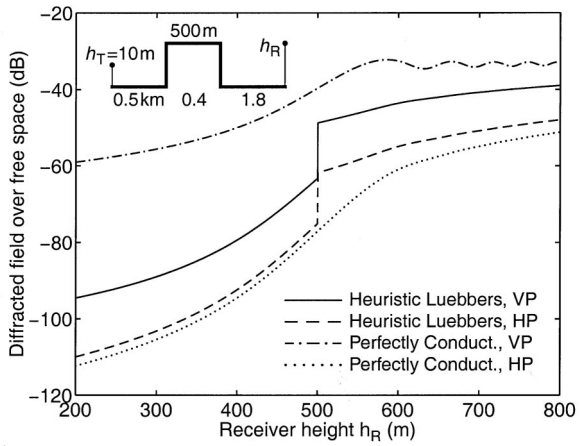

Fig. 4. Diffracted field for a spherical source in the presence of two joined $n = 3/2$ wedges when using a factor of 1/2 for grazing incidence. The frequency is 300 MHz, the relative permittivity $\epsilon_r = 15$, and the conductivity $\sigma = 0.012$ S/m.

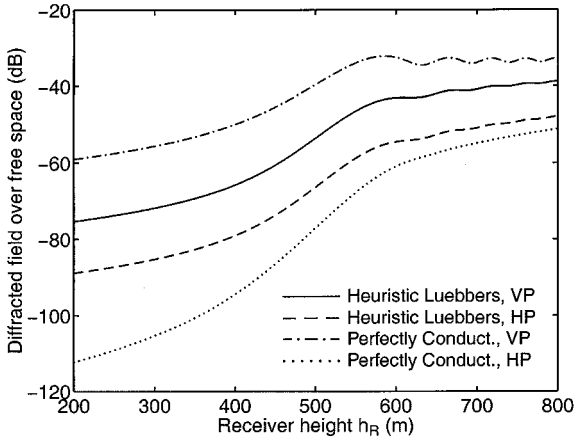

Fig. 5. As in Fig. 4, except for the use of the approach for grazing incidence in [22].

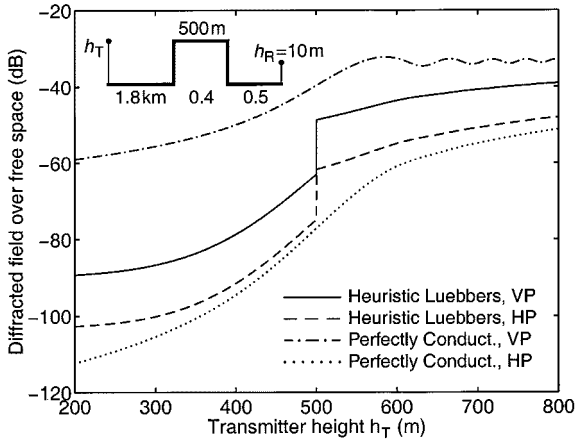

Fig. 6. As in Fig. 5, when turning around the height profile and varying the transmitter height.

extension for nonperfectly conducting faces is made. The coefficients R_0 and R_n in (1) are simply replaced by proper Fresnel plane wave reflection coefficients and surface roughness attenuation factors. Here, this heuristic approach will be considered. However, in order to get a result for a single wedge that corresponds to the solution by Maliuzhinets [8], we will only use the Fresnel plane wave reflection coefficient; no surface roughness will be considered. In addition, the surface roughness attenuation factor does not follow from Maxwell's equations.

The heuristic coefficient by Luebbers [3] works very well in the vicinity of the reflection boundaries, but not deep in the shadow region [16], [17], [21]. In [22], that coefficient is applied to diffraction by two joined wedges. Diffraction by two joined wedges will also be considered here but without a surface roughness attenuation factor. Furthermore, in [22], first- and second-order diffracted fields are used, i.e., the terms $m = 0$ and $m = 1$ in (10). We will use terms up to $m = 2$. When dealing with multiple diffraction, higher order diffracted fields might be required for a good result and, depending on the diffraction geometry, terms up to order 2 might not be sufficient. For the double-diffraction examples in this paper, however, the first- and the second-order field give good enough results. Also, when using Fresnel plane wave reflection coefficient, derivatives of the reflection coefficients have to be elaborated [22], which is cumbersome for large m.

In Fig. 4, we have used the heuristic coefficient by Luebbers [3] together with a factor of 1/2 for grazing incidence. The diffraction geometry in Fig. 4 is the one used in [22] (Figs. 2 and 3). The result is discontinuous. (For a single wedge, the coefficient by Luebbers always gives a continuous result, at least for an exterior wedge.) Obviously, the factor of 1/2 used to deal with grazing incidence does not work for nonperfectly conducting surfaces.

In [22], the above problem was solved by introducing gain factors, where a gain factor is equal to the ratio of the incident field to an incident-plus-reflected field. The introduction is reasonable, as the gain factors are in line with the origin of the factor of 1/2 in the perfectly conducting case [1], [7]. Furthermore, these factors are only applied to the first-order diffracted field. For the slope diffraction term (the term $m = 1$), the usual factor of 1/2 is used and, in our case, also for the third-order diffracted field (the term $m = 2$). The result, which is shown in Fig. 5, is continuous and smooth. Now, if we use this approach for grazing incidence but turn around the height profile and vary the transmitter height instead, we should end up with the same result as in Fig. 5. However, this is not the case, as can be seen in Fig. 6. The result is not only different from the one in Fig. 5, it is also discontinuous. Evidently, the approach for grazing incidence in [22] does not necessarily give continuous nor reciprocal results. Luebbers coefficient in [3] used together with a factor of 1/2, on the other hand, gives reciprocal, but not continuous, results. (If Luebbers coefficient is used together with a factor of 1/2 for the diffraction geometry in Fig. 6, the result will be the same as the one in Fig. 4.) Thus, there is more to the problem than altering the factor of 1/2. Note: Figs. 4–6 show only diffracted fields, no reflections are considered, i.e., the reflections from the horizontal segments near the antennas are neglected (which also is done in [22]).

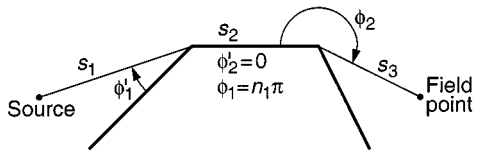

Fig. 7. Ray geometry for diffraction by two joined wedges.

Due to the findings above, let us see what happens in the vicinity of the shadow boundary when using a factor of 1/2 for grazing incidence and when using the gain factors introduced in [22]. In the vicinity of the shadow boundary, the height h_{R} in Fig. 4 or 5, is close to 500 m. Considering Fig. 7, if we put the reflection coefficients associated with the double diffraction by the two wedges to $R_{0,1}(\phi_1') = R_1$, $R_{n,1}(n_1\pi - \phi_1 = 0) = R_2 = -1$, $R_{0,2}(\phi_2' = 0) = R_2 = -1$, and $R_{n,2}(n_2\pi - \phi_2) = R_3$, where the arguments of the reflection coefficients follow from Fig. 2, the two diffraction coefficients for the doubly diffracted ray in Fig. 7 can be written as

$$\begin{aligned} D_1 &= D(L_1, n_1; \phi_1 = n_1\pi, \phi_1') \\ &= (1+R_2)\, D_1^{(1,4)} + (1+R_1)\, D_1^{(2,3)} \end{aligned} \tag{11}$$

and

$$\begin{aligned} D_2 &= D(L_2, n_2; \phi_2, \phi_2' = 0) \\ &= (1+R_2)\, D_2^{(1,3)} + (1+R_3)\, D_2^{(2,4)} \end{aligned} \tag{12}$$

where $L_1 = s_1 s_2/(s_1+s_2)$, $L_2 = s_2 s_3/(s_2+s_3)$ and the arguments of $D_i^{(l)}$ ($l = 1, 2, 3, 4$; $i = 1, 2$) are omitted and assumed to be understood. Furthermore, here the notation $D_1^{(1,4)}$, for instance, simply means that either $D_1^{(1)}$ or $D_1^{(4)}$ can be used as $D_1^{(1)} = D_1^{(4)}$ for the diffraction geometry in Fig. 7.

The case that we are interested in is when $\phi_1' < n_1\pi - \pi$ and $\phi_2 \approx \pi$, as that corresponds to the height $h_{\mathrm{R}} \approx 500$ m in Fig. 4 or 5. For the sake of simplicity, let us assume that $s_2 \gg s_1$, s_3 (which really is not true for the height profiles in Figs. 4 and 5) and approximate (12) by

$$\begin{aligned} D_2 &\approx D(L_2 \approx s_3, n_2; \phi_2 \approx \pi, \phi_2' = 0) \\ &\approx \begin{cases} (1+R_3)\, D_2^{(2,4)} - \dfrac{1}{2}(1+R_2)\sqrt{s_3}, & \text{for } \phi_2 < \pi \\ (1+R_3)\, D_2^{(2,4)} + \dfrac{1}{2}(1+R_2)\sqrt{s_3}, & \text{for } \phi_2 \geq \pi \end{cases} \end{aligned} \tag{13}$$

which, when considering (9), gives the approximate first-order field

$$E_{\mathrm{UTD}}^{1/2} \approx \frac{E_0 e^{-jks_{\mathrm{T}}}}{s_{\mathrm{T}}} \frac{D_1}{2\sqrt{s_1 s_3}}\,(1+R_3)\, D_2^{(2,4)} \tag{14}$$

for the doubly diffracted ray when using a factor of 1/2 for grazing incidence and when using $R_2 = -1$, where D_1 stands for $D(L_1 \approx s_1, n_1; \phi_1 = n_1\pi, \phi_1')$. If we use the approach by Luebbers for grazing incidence [22], this approximate field becomes

$$\begin{aligned} E_{\mathrm{UTD}}^{\mathrm{L}} \approx \frac{E_0 e^{-jks_{\mathrm{T}}}}{s_{\mathrm{T}}} \frac{D_1}{2\sqrt{s_1 s_3}} \\ \cdot \begin{cases} (1+R_3)\, D_2^{(2,4)} - \sqrt{s_3}, & \text{for } \phi_2 < \pi \\ (1+R_3)\, D_2^{(2,4)} + \sqrt{s_3}, & \text{for } \phi_2 \geq \pi. \end{cases} \end{aligned} \tag{15}$$

Besides a doubly diffracted ray, we also have a singly diffracted ray for $\phi_2 < \pi$ with the diffraction coefficient $D(L, n_1; \phi, \phi' = \phi_1')$, where $L = s's/(s'+s)$ and $s' = s_1$. Furthermore, considering Fig. 7, for $\phi_2 \approx \pi$, i.e., for $\phi \approx n_1\pi$, we know that $s \approx s_2 + s_3$, which means that $L \approx s_1$ when $s_2 \gg s_1, s_3$. Consequently, for $s_2 \gg s_1, s_3$ and $\phi_2 \approx \pi$, the coefficient for the singly diffracted ray can be written approximately as $D(s_1, n_1; n_1\pi, \phi_1') \approx D_1$, which, according to (5) gives the approximate field

$$E_{\mathrm{UTD}} \approx \frac{E_0 e^{-jks_{\mathrm{T}}}}{s_{\mathrm{T}}} \frac{D_1}{\sqrt{s_1}} \cdot \begin{cases} 1, & \text{for } \phi_2 < \pi \\ 0, & \text{for } \phi_2 \geq \pi \end{cases} \tag{16}$$

for the singly diffracted ray. (Note: In order to avoid a sharp peak at the shadow boundary of the second wedge, the appearance of the singly diffracted ray has to occur exactly when the diffraction coefficient of the second wedge changes sign. Here, there are two possibilities; this may be allowed to occur when $\phi_2 < \pi$ or when $\phi_2 \leq \pi$. In [18], we use the latter definition. In this paper, we use the former one, as it seems to be the one most frequently used.)

Now, with respect to the fields in (14) to (16), obviously the approach by Luebbers for grazing incidence gives approximately a continuous first-order field across the shadow boundary, i.e., (15)+(16) gives approximately a continuous field across the shadow boundary, while the factor of 1/2 does not, i.e., (14)+(16) does not. However, both approaches give first-order diffracted fields that are nonzero in the shadow region, which is not expected. Considering the result of the more rigorous solution for diffraction by a single nonperfectly conducting wedge in reference [9] by Tibero *et al.*, except for vertical (hard) polarization and perfectly conducting surfaces, the diffracted field vanishes on the surface. Consequently, the field diffracted by the first wedge and which incident on the second wedge should be zero. In other words, the diffraction coefficient D_1 in (11) should be zero for $R_2 = -1$. Thus, for double diffraction by two joined nonperfectly conducting wedges, the first-order diffracted field is expected to be zero in both polarization cases, contrary to perfectly conducting wedges, where only horizontal (soft) polarization gives a zero first-order field. In addition, for two joined wedges with nonperfectly conducting faces, this means that it has to be the diffracted fields of second-order and higher that give rise to a nonzero doubly diffracted field.

There are clearly problems associated with the heuristic coefficient by Luebbers. For instance, it overestimates the field strength in shadow region [16], [17] and for two joined wedges (when using a factor of 1/2 for grazing incidence), it gives a discontinuous result at the shadow boundary, problems to which the approach in [22] offers no solution.

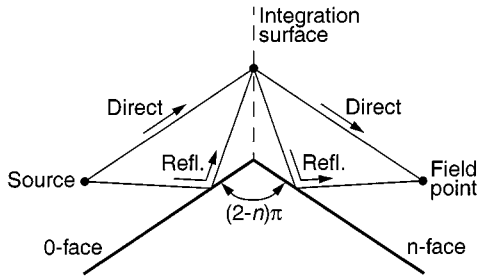

Fig. 8. Illustration of the Fresnel–Kirchhoff theory applied to a noncurved wedge.

IV. New Heuristic Diffraction Coefficient

Considering the diffraction coefficient in (1), one may note that there are no shadow boundaries for $n < 1$. In this case, the first two terms in (1) are associated with double-reflection boundaries. The first has a boundary of an incident field first reflected from the n-face and then from the zero-face, whereas the second has a boundary of an incident field first reflected from the zero-face and then from the n-face. In line with the heuristic diffraction coefficient by Luebbers [3], this means that D in (1) would read as $R_0R_nD^{(1)}+R_0R_nD^{(2)}+R_0D^{(3)}+R_nD^{(4)}$ for an interior wedge. For perfectly conducting surfaces, the factor R_0R_n will always be equal to $+1$ both for soft and hard polarizations. However, assuming that the heuristic approach by Luebbers [3] is valid, this will not be the case for nonperfectly conducting wedge faces. This factor, which will be important in this section, can assume other values than one here.

For scattering in the forward direction, the Fresnel–Kirchhoff theory can be used for diffraction by a wedge [23], [24]. Considering Fig. 1, assuming perfectly conducting surfaces and that $s'k,\ sk \gg 1$, for n close to one and $(\phi - \phi')$ close to π, it can be shown that the Fresnel–Kirchhoff theory gives a result comparable to more rigorous solutions [23]. In Fig. 8, the use of this theory is illustrated for diffraction by a noncurved wedge. The field can be divided into four parts, one direct–direct, one reflected–reflected, one reflected–direct, and one direct–reflected. In a UTD context, this would correspond to the following proposed new heuristic diffraction coefficient:

$$\begin{aligned} D &= D(L,\, n;\, \phi,\, \phi') \\ &= D^{(1)} + R_0R_nD^{(2)} + R_0D^{(3)} + R_nD^{(4)}. \end{aligned} \tag{17}$$

This new coefficient is an extension of the one in [3] and is as simple to compute. Furthermore, with restriction to scattering in the forward direction, the coefficient in (17) would be valid both for $n > 1$ and $n < 1$, as the above comparison is possible both for $n > 1$ and $n < 1$. Thus, no matter whether the wedge is an exterior or an interior one, the four components in (17) should be associated with the boundaries of the four possible rays in the presence of a wedge, i.e., the boundaries of a direct ray, a doubly reflected ray, and two singly reflected rays. In the following text, the validity of the new coefficient, especially when n is greater than one, is discussed.

For $n < 1$, it is justified to put the factor $R_0(\phi')R_n(n\pi - \phi)$ in front of the component $D^{(2)}$, where the arguments of the reflection coefficients follow from Fig. 1. The issue here, however, is whether the component $D^{(1)}$ should be multiplied by this factor or not. As it is associated with the double-reflection boundary of a field incidenting opposite to the forward direction, it should be multiplied by the factor $R_0(\phi)R_n(n\pi - \phi')$ and not $R_0(\phi')R_n(n\pi-\phi)$. On the other hand, for forward-scattering, the component $D^{(1)}$ will stand for a contribution that is small, at least if one considers that $n < 1$ means that we are always in the lit region. Thus, for $n < 1$ and forward scattering, the coefficient in (17) is a reasonable solution in line with the heuristic coefficient by Luebbers.

For the other case, i.e., $n > 1$, it does not seem to be justified to put the factor $R_0(\phi')R_n(n\pi-\phi)$ in front of $D^{(2)}$. Here, $D^{(2)}$ is associated with the shadow boundary of a field incidenting opposite to the forward direction. For forward scattering, $D^{(2)}$ will always stand for a small contribution. However, that is also the case for the other diffraction components in the shadow region. Thus, we have here a region where it is possible to test the coefficient in (17). Furthermore, it is the region where a better heuristic solution than the previous one by Luebbers is desired.

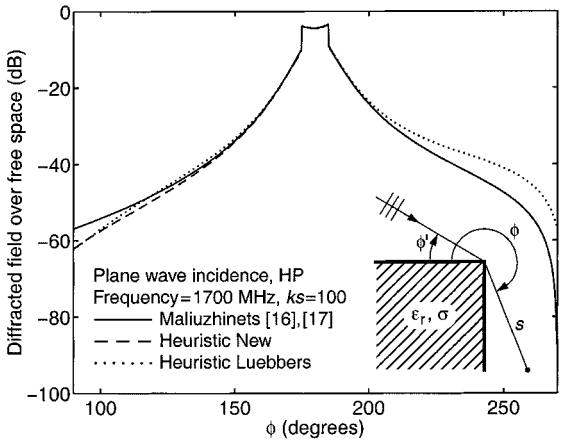

Fig. 9. Diffracted field for an incident plane wave in the presence of a $n = 3/2$ wedge. The angle $\phi' = 5°$, the relative permittivity $\epsilon_r = 8$, and the conductivity $\sigma = 0.001$ S/m.

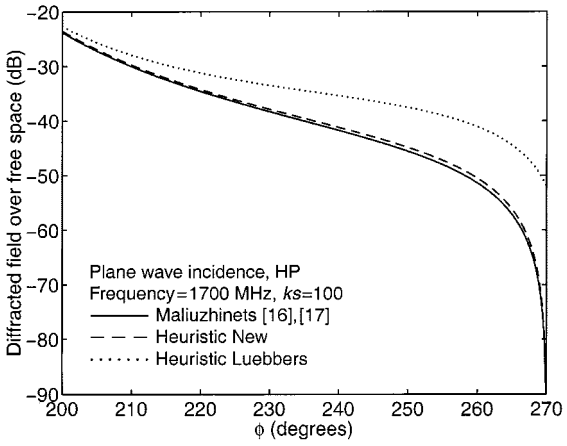

Fig. 10. As in Fig. 9, except for the relative permittivity $\epsilon_r = 3$ and the conductivity $\sigma = 0.002$ S/m.

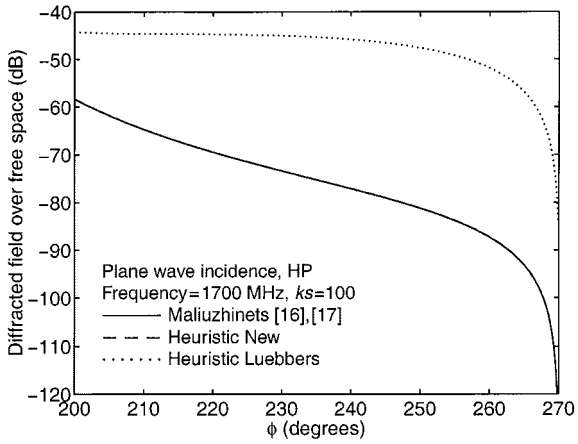

Fig. 11. As in Fig. 9, except for the angle $\phi' = 0.1°$ and the conductivity $\sigma = 0.002$ S/m.

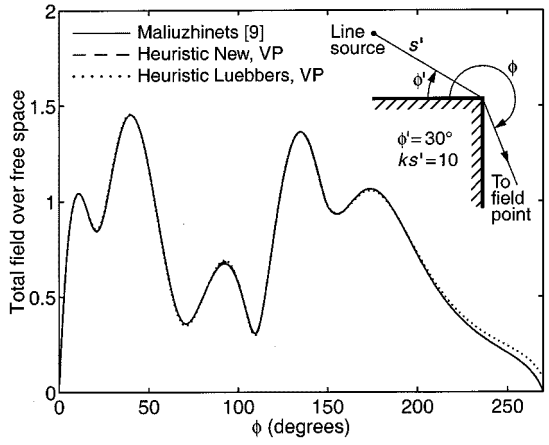

Fig. 12. Total far field for a line source in the presence of an $n = 3/2$ wedge with equal face impedances.

A first indication that (17) might provide a better result than the previous one is seen when the diffraction coefficients in (11) and (12) are written down using (17). For (17), these coefficients read as

$$D_1 = (1+R_2)\left(D_1^{(1,4)} + R_1 D_1^{(2,3)}\right) \tag{18}$$

and

$$D_2 = (1+R_2)\left(D_2^{(1,3)} + R_3 D_2^{(2,4)}\right). \tag{19}$$

Here, the expression for D_1 yields that a singly diffracted field vanishes on the wedge surface as $R_2 = -1$. This is a desired property, which thus gives a zero first-order diffracted field for two joined wedges. Furthermore, it also makes the approach for grazing incidence in [22] unnecessary, as the proposed gain factors in [22] are only applied to first-order diffracted fields, i.e., we are back to the use of a factor of 1/2 for grazing incidence.

Now, the really interesting results are revealed when (17) is used to calculate the diffracted fields for some examples showing results based on Maliuzhinets's solution without surface wave effects [9], [16], [17]. In Figs. 9–12, the new and the old heuristic coefficient can be compared with these more rigorous solutions. The new coefficient gives results surprisingly close to the ones based on Maliuzhinets's solution, while the old one does not, at least not in the shadow regions; see also [25]. Note: In Figs. 9–11, the solution given in [16] and [17] has been used for $\sin\theta_{0,n} = \sqrt{\epsilon}$, which corresponds to one over the normalized surface impedance for horizontal polarization at normal incidence. Here, ϵ is the complex relative permittivity, i.e., $\epsilon = \epsilon_r - j\sigma/\omega\epsilon_0$. In Fig. 12, the solution given in [9] has been used for $\sin\theta_{0,n} = 0.25 = 1/\sqrt{\epsilon}$, which corresponds to the normalized surface impedance for vertical polarization at normal incidence.

It may be noted that none of Figs. 9–11 show a result for angles below 90°, i.e., $\phi = \pi/2$, as the argument in $R_n(n\pi - \phi) = R_n(3\pi/2 - \phi)$ would then exceed the grazing angle π, which has no meaning. Moreover, it is in the backscattering region, which is not of interest in this paper. However, for ϕ' above $(n-1/2)\pi$, it should be possible to obtain good results for ϕ below $\pi/2$ by using the diffraction coefficient $R_0(\phi)R_n(n\pi - \phi')D^{(1)} + D^{(2)} + R_0(\phi)D^{(3)} + R_n(n\pi - \phi')D^{(4)}$. What happens in between, on the other hand, is hidden in Maliuzhinets's solution.

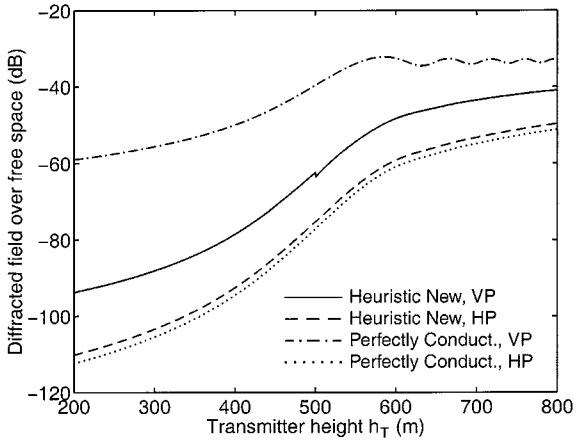

Fig. 13. As in Fig. 6, except for the use of the new heuristic diffraction coefficient in (17) for nonperfectly conducting surfaces and a factor of 1/2 for grazing incidence.

In Fig. 9, one can see that both the new and the old coefficient start to give bad results when the angle ϕ approaches 90°. However, if the geometrical optics field is added, this failure of the heuristic coefficients might not show. In Fig. 12, the geometrical optics field dominates in the lit region. Consequently, here the new coefficient give good results within the whole range of angles, from 0° to 270°.

For the diffraction example in Fig. 6, we obtained discontinuous results. If we perform the same calculation as in Fig. 6, but for the new heuristic coefficient in (17), we end up with the result shown in Fig. 13. The discontinuities are gone, besides a small one for vertical polarization. Furthermore, if we use (17) for the diffraction geometry in Fig. 4 (or Fig. 5), the result will be exactly the same as in Fig. 13, including the small discontinuity for vertical polarization. This is very important as it means that (17) is able to provide a reciprocal result.

Turning back to the small discontinuity for vertical polarization in Fig. 13, it cannot be removed by adding more higher order terms. (For all doubly diffracted fields, we use terms up to

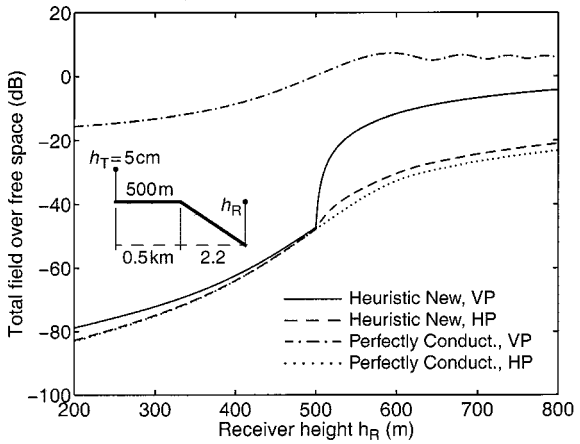

Fig. 14. Total field for a spherical source in the presence of a wedge. The frequency is 300 MHz, the relative permittivity $\epsilon_r = 15$, and the conductivity $\sigma = 0.012$ S/m. The total path distance is 2.7 km and the transmitter is 5 cm above the first face.

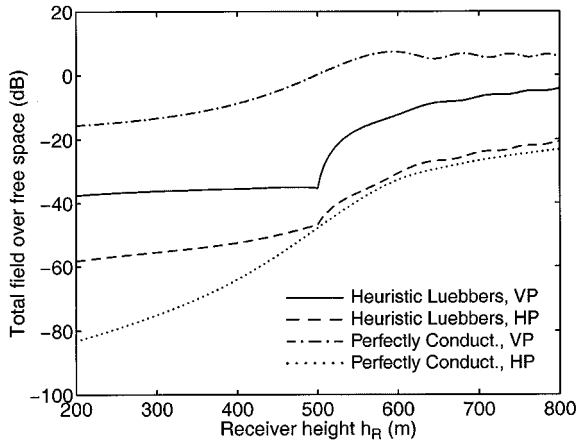

Fig. 15. As in Fig. 14, except for the use of the heuristic coefficient by Luebbers [3].

$m = 2$ and the term $m = 2$ improves the result very little.) Here, we have a failure that is due to the heuristic approach in finding (17). In Fig. 14, the failure should be obvious. The results in the nonperfectly conducting case are continuous but with discontinuous slopes. For small grazing angles and vertical polarization, the reflection coefficient varies rapidly as the angle varies, and in Fig. 14, a reflection with a rapid varying coefficient appears at the height $h_R = 500.22$ m. Consequently, the expression in (17) gives a continuous result but does not account for varying reflection coefficients in a proper way, which, in this case, results in a small slope discontinuity for vertical polarization in Fig. 13.

The above problem is also something that the expression by Luebbers in [3] suffers from, as can be seen in Fig. 15. Of course, this is expected, as the coefficient in (17) is simply an extension of the one in [3]. In Fig. 5, however, as the approach for grazing incidence in [22] gives a nonzero first-order field, it does not show. On the other hand, for a larger transmitter height, we will end up closer to a region of overlapping transition regions,

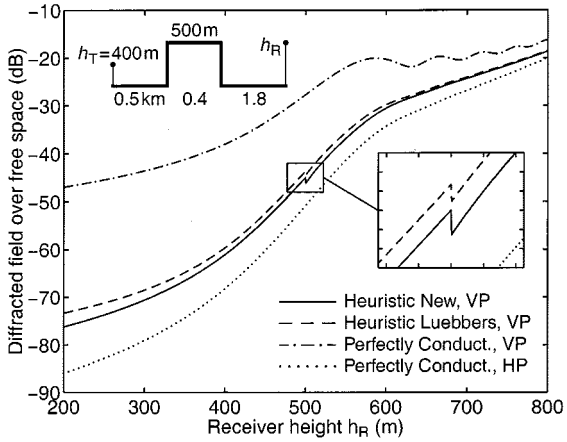

Fig. 16. Diffracted field for a spherical source in the presence of two joined $n = 3/2$ wedges. The new heuristic coefficient in (17) is used together with a factor of 1/2 for grazing incidence. The old is used together with the approach for grazing incidence in [22]. The frequency is 300 MHz, the relative permittivity $\epsilon_r = 15$, and the conductivity $\sigma = 0.012$ S/m. The x- and the y-grid in the small figure are 10 m and 1 dB, respectively.

which means that the slope diffraction term will become more important and the discontinuity of the coefficient in [3] might become visible. This is what happens in Fig. 16, where the discontinuities of the new heuristic coefficient in (17) and the one in [3] are about 1.5 and 1 dB, respectively. Thus, both the new and the old coefficient fail to some extent when a rapid varying reflection coefficient is involved.

The results in the nonperfectly conducting case in Fig. 13 are obtained using derivatives of the reflection coefficients. If we use higher order terms without making use of the derivatives of the reflection coefficients, these results will be worse. In fact, they will be very similar to the ones in Fig. 14, i.e., continuous but with discontinuous slopes. Consequently, even though (17) does not account for varying reflection coefficients in a proper way, it is not completely wrong. Moreover, if the thickness of the ridge is increased, the small discontinuity for the vertical polarization decreases and for a ridge thickness of 4 km, i.e., $s_2 = 4$ km, it is almost gone. Furthermore, an increase in the first distance of the height profile in Fig. 14 will also give a better result, as can be seen in Fig. 17, where the results of the new and old coefficients are shown for vertical polarization and for the same grazing angle, i.e., the same angle ϕ', as in Figs. 14 and 15. Here, the large distance to the wedge means that we have an approximate incident plane wave. Thus, rapid varying reflection coefficients cause errors. However, if the separation distances between the source, the wedge or the wedges, and the field point are large enough, the errors will be small.

V. Conclusion

An extension of the heuristic diffraction coefficient by Luebbers, which, at least, is valid for scattering in the forward direction, has been proposed. When neglecting surface waves, the new heuristic coefficient gives results in good agreement with what the more exact diffraction coefficient by Maliuzhinets gives, even deep in the shadow region, where the previous coefficient fails. Even so, it is as simple as the previous one to

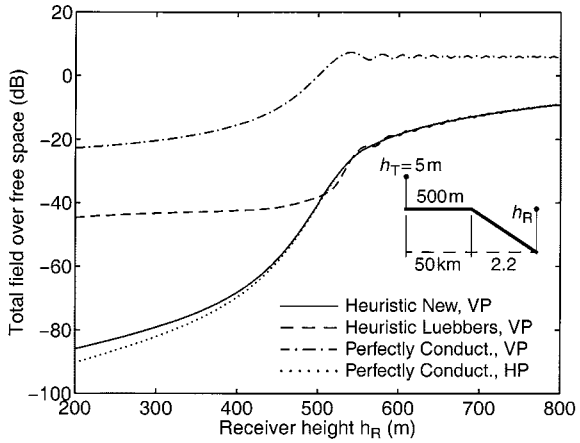

Fig. 17. Total field for a spherical source in the presence of a wedge. The frequency is 300 MHz, the relative permittivity $\epsilon_r = 15$, and the conductivity $\sigma = 0.012$ S/m. The total path distance is 52.2 km and the transmitter is 5 m above the first face.

compute. Moreover, it does not require any special care when grazing incidence occurs, i.e., the usual factor of 1/2 can be used.

The new coefficient works very well for incident plane waves, which is not unexpected as the reflection coefficients used are for plane waves. For a wedge illuminated by a spherical source, however, problems might arise. Here, reflection coefficients with rapid spatial variations can be involved, which causes errors. This is also a problem of the old coefficient and is hard to do anything about. However, if the separation distances between the source, the wedge or the wedges and the field point are large enough, the errors will be small.

APPENDIX

Considering the doubly diffracted ray in Fig. 2, provided that we have forward scattering and are well outside the reflection transition regions, the field in (10) can approximately be written as

$$E_{\mathrm{UTD}} \approx \frac{E_0 e^{-jks_{\mathrm{T}}}}{s_{\mathrm{T}}} \sqrt{\frac{s_{\mathrm{T}}}{s_1 s_2 s_3}} \sum_{m=0}^{\infty} \frac{1}{m!} \left(\frac{-1}{jks_2}\right)^m \cdot \frac{\partial^m D_1^{(1)}}{\partial \phi_1^m} \frac{\partial^m D_2^{(1)}}{\partial \phi_2'^m} \tag{20}$$

for overlapping shadow transition regions, where the derivatives $\partial^m D_1^{(1)}/\partial \phi_1^m$ and $\partial^m D_2^{(1)}/\partial \phi_2'^m$ follow from [18] and read as

$$\frac{\partial^m D_1^{(1)}}{\partial \phi_1^m} = \frac{-e^{-j\pi/4}}{2n_1\sqrt{2\pi k}} F_m\left(2kL_1 n_1^2 \sin^2 \gamma_1^{(1)}\right) \frac{\partial^m}{\partial \phi_1^m} \cot \gamma_1^{(1)} \tag{21}$$

and

$$\frac{\partial^m D_2^{(1)}}{\partial \phi_2'^m} = \frac{-e^{-j\pi/4}}{2n_2\sqrt{2\pi k}} F_m(2kL_2 n_2^2 \sin^2 \gamma_2^{(1)}) \frac{\partial^m}{\partial \phi_2'^m} \cot \gamma_2^{(1)} \tag{22}$$

where

L_1 $s_1 s_2/(s_1 + s_2)$;
$\gamma_1^{(1)}$ $[\pi - (\phi_1 - \phi_1')]/2n_1$;
L_2 $s_2 s_3/(s_2 + s_3)$;
$\gamma_2^{(1)}$ $[\pi - (\phi_2 - \phi_2')]/2n_2$; and
F_m transition function of order m introduced in [18].

For overlapping shadow transition regions, both the angles $\gamma_1^{(1)}$ and $\gamma_2^{(1)}$ will be close to zero, a case that we will take a closer look at here. Furthermore, for overlapping shadow transition regions, the arguments of the above transition functions will be small. Using [18], for a very small argument x in $F_m(x)$, it can be shown that

$$F_m(x) \approx \frac{(2jx)^{m/2}}{m!!} \cdot \begin{cases} \sqrt{\pi x} e^{j\pi/4}, & \text{for } m = 0, 2, 4, \ldots \\ \sqrt{2x} e^{j\pi/4}, & \text{for } m = 1, 3, 5, \ldots \end{cases} \tag{23}$$

which gives the usable limit

$$\lim_{\gamma \to \pm 0} F_m\left(\alpha \sin^2 \gamma\right) \frac{d^m}{d\gamma^m} \cot \gamma = \frac{m!(2j\alpha)^{m/2}}{m!!} \cdot \begin{cases} \pm\sqrt{\pi\alpha} e^{j\pi/4}, & \text{for } m = 0, 2, 4, \ldots \\ -\sqrt{2\alpha} e^{j\pi/4}, & \text{for } m = 1, 3, 5, \ldots \end{cases}. \tag{24}$$

Now, let us consider the case where the doubly diffracted ray is the only one existing. In other words, let us consider the case when $\gamma_1^{(1)} \to -0$ and $\gamma_2^{(1)} \to -0$. Using (24), in the limits $\gamma_1^{(1)} \to -0$ and $\gamma_2^{(1)} \to -0$, (21) and (22) result in

$$\lim_{\gamma_1^{(1)} \to -0} \frac{\partial^m D_1^{(1)}}{\partial \phi_1^m} = \frac{m!(jkL_1)^{m/2}}{m!!} \frac{\sqrt{L_1}}{2} \cdot \begin{cases} 1, & \text{for } m = 0, 2, 4, \ldots \\ -\sqrt{2/\pi}, & \text{for } m = 1, 3, 5, \ldots \end{cases} \tag{25}$$

and

$$\lim_{\gamma_2^{(1)} \to -0} \frac{\partial^m D_2^{(1)}}{\partial \phi_2'^m} = \frac{m!(jkL_2)^{m/2}}{m!!} \frac{\sqrt{L_2}}{2} \cdot \begin{cases} 1, & \text{for } m = 0, 2, 4, \ldots \\ \sqrt{2/\pi}, & \text{for } m = 1, 3, 5, \ldots \end{cases} \tag{26}$$

respectively, as $\partial/\partial\phi_1 = (-1/2n_1)\partial/\partial\gamma_1^{(1)}$ and $\partial/\partial\phi_2' = (1/2n_2)\partial/\partial\gamma_2^{(1)}$. These last two equations make it possible to write approximately the field in (20) in the compact form

$$E_{\mathrm{UTD}} \approx \frac{E_0 e^{-jks_{\mathrm{T}}}}{s_{\mathrm{T}}} \sqrt{\frac{s_{\mathrm{T}} L_1 L_2}{s_1 s_2 s_3}} \sum_{m=0}^{\infty} \frac{a_m m!}{(m!!)^2} \left(\frac{L_1 L_2}{s_2^2}\right)^{m/2} \tag{27}$$

where

$$a_m = \begin{cases} 1/4, & \text{for } m = 0, 2, 4, \ldots \\ 1/(2\pi), & \text{for } m = 1, 3, 5, \ldots \end{cases} \tag{28}$$

which, finally, can be rewritten as

$$E_{\mathrm{UTD}} \approx \frac{E_0 e^{-jks_{\mathrm{T}}}}{s_{\mathrm{T}}} \sqrt{\frac{s_{\mathrm{T}}}{s_1 s_2 s_3}} \left[\frac{\sqrt{L_1 L_2}}{4} + \frac{\sqrt{L_1 L_2}}{4} \cdot \sum_{m=1}^{\infty} \left(\frac{(2m-1)!!}{(2m)!!} + \frac{2s_2/\pi}{\sqrt{L_1 L_2}} \frac{(2m-2)!!}{(2m-1)!!} \right) x^m \right] \tag{29}$$

where

$$x = \frac{L_1 L_2}{s_2^2} = \frac{s_1 s_3}{(s_1 + s_2)(s_2 + s_3)}. \tag{30}$$

The approximate field in (29) is thus only valid when the source and the field point are immediately below the straight line formed by the two wedges. In addition, in order for the approximation to be accurate, we have to be well outside the reflection transition regions.

As far as the convergence is concerned, the series in (29) will always converge. The factors $(2m-1)!!/(2m)!!$ and $(2m-2)!!/(2m-1)!!$ are less than or equal to one, so the convergence of the series can be assured by comparing it with a geometric series with quotient x. Thus, since x will always be smaller than one (except for $s_2 = 0$), the series will always converge and the convergence will be fast if $s_2 \gg s_1, s_3$. If $s_2 \ll s_1, s_3$, on the other hand, the convergence will be very slow as x will be close to one. In addition, it may be noted that the convergence does not depend on the wavelength; it is the mutual relations between s_1, s_2, and s_3 that determine the convergence.

REFERENCES

[1] D. A. McNamara, C. W. I. Pistorius, and J. A. G. Malherbe, *Introduction to the Uniform Geometrical Theory of Diffraction*. Norwood, MA: Artech House, 1990.

[2] K. A. Chamberlin and R. J. Luebbers, "An evaluation of longley-rice and GTD propagation models," *IEEE Trans. Antennas Propagat.*, vol. AP-30, pp. 1093–1098, Nov. 1982.

[3] R. J. Luebbers, "Finite conductivity uniform GTD versus knife edge diffraction in prediction of propagation path loss," *IEEE Trans. Antennas Propagat.*, vol. AP-32, pp. 70–76, Jan. 1984.

[4] ——, "Propagation prediction for hilly terrain using GTD wedge diffraction," *IEEE Trans. Antennas Propagat.*, vol. AP-32, pp. 951–955, Sept. 1984.

[5] K. A. Chamberlin, "An automated approach for implementing GTD to model 2-D terrain effects at microwave frequencies," *IEEE Trans. Electromagn. Compat.*, vol. 21, pp. 7–14, Feb. 1996.

[6] J. B. Keller, "Geometrical theory of diffraction," *J. Opt. Soc. Amer.*, vol. 52, no. 2, pp. 116–130, Feb. 1962.

[7] R. G. Kouyoumjian and P. H. Pathak, "A uniform geometrical theory of diffraction for an edge in a perfecly conducting surface," *Proc. IEEE*, vol. 62, pp. 1448–1461, Nov. 1974.

[8] G. D. Maliuzhinets, "Excitation, reflection and emission of surface waves from a wedge with given face impedances," *Sov. Phys. Dokl.*, vol. 3, no. 4, pp. 752–755, 1958.

[9] R. Tiberio, G. Pelosi, and G. Manara, "A uniform GTD formulation for the diffraction by a wedge with impedance faces," *IEEE Trans. Antennas Propagat.*, vol. AP-33, pp. 867–873, Aug. 1985.

[10] R. G. Rojas, "Electromagnetic diffraction of an obliquely incident plane wave field by a wedge with impedance faces," *IEEE Trans. Antennas Propagat.*, vol. 36, pp. 956–970, July 1988.

[11] R. Tiberio, G. Pelosi, G. Manara, and P. H. Pathak, "High-frequency scattering from a wedge with impedance faces illuminated by a lina source—Part I: Diffraction," *IEEE Trans. Antennas Propagat.*, vol. 37, pp. 212–218, Feb. 1989.

[12] ——, "High-frequency scattering from a wedge with impedance faces illuminated by a lina source, Part II: Surface waves," *IEEE Trans. Antennas Propagat.*, vol. 41, pp. 877–883, July 1993.

[13] G. Pelosi, G. Manara, and P. Nepa, "Diffraction by a wedge with variable-impedance faces," *IEEE Trans. Antennas Propagat.*, vol. 44, pp. 1334–1340, Oct. 1996.

[14] M. F. Otero and R. G. Rojas, "Two-dimensional Green's function for a wedge with impedance faces," *IEEE Trans. Antennas Propagat.*, vol. 45, pp. 1799–1809, Dec. 1997.

[15] R. J. Luebbers, "Comparison of lossy wedge diffraction coefficients with application to mixed path propagation loss prediction," *IEEE Trans. Antennas Propagat.*, vol. 36, pp. 1031–1034, July 1988.

[16] C. Bergljung and L. G. Olsson, "Rigorous diffraction theory applied to street microcell propagation," in *Proc. IEEE Global Telecommun. Conf.*, Phoenix, AZ, Dec. 1991, pp. 1292–1296.

[17] C. Bergljung, "A comparison of solutions to the problem of diffraction of plane wave by a dielectric wedge," in *Proc. Nordic Radio Symp.*, Aalborg, Denmark, June 1992, pp. 43–46.

[18] P. D. Holm, "UTD-diffraction coefficients for higher order wedge diffracted fields," *IEEE Trans. Antennas Propagat.*, vol. 44, pp. 879–888, June 1996.

[19] K. R. Jakobsen, "An alternative diffraction coefficient for the wedge," *IEEE Trans. Antennas Propagat.*, vol. AP-32, pp. 175–177, Feb. 1984.

[20] Y. Liu and I. R. Ciric, "Improved formulas for the diffraction by a wedge," *Radio Sci.*, vol. 28, no. 5, pp. 859–863, Sept./Oct. 1993.

[21] C. Demeterscu and C. C. Constantinou, "Scattering by a right-angled lossy dielectric wedge," *Proc. Inst. Elect. Eng. Microwave Antennas Propagat.*, vol. 144, no. 5, pp. 392–396, Oct. 1997.

[22] R. J. Luebbers, "A heuristic UTD slope diffraction coefficient for rough lossy wedges," *IEEE Trans. Antennas Propagat.*, vol. 37, pp. 206–211, Feb. 1989.

[23] J. H. Whitteker, "Fresnel–Kirchhoff theory applied to terrain diffraction problems," *Radio Sci.*, vol. 25, no. 5, pp. 837–851, Sept./Oct. 1990.

[24] ——, "A series solution for diffraction over terrain modeled as multiple bridged knife edges," *Radio Sci.*, vol. 28, no. 4, pp. 487–500, July/Aug. 1993.

[25] P. D. Holm, "An extension of a heuristic UTD diffraction coefficient for nonperfectly conducting wedges," in *Proc. Nordic Radio Symp.*, Saltsjöbaden, Sweden, Oct. 1998, pp. 75–78.

Peter D. Holm was born in Boden, Sweden. He received the M.Sc. degree in physics and the Ph.D. degree in theoretical physics both from the University of Linköping, Sweden, in 1982 and 1989, respectively.

Since 1990, he has been with the Department of Communication Systems, Division of Command and Control Warfare Technology, National Defence Research Establishment, Linköping, Sweden, where he has been involved with electromagnetic wave propagation problems. His current research interest is radio wave propagation modeling over irregular terrain.